PHYSICAL REVIEW C **70**, 031601(R) (2004)

Interplay of initial deformation and Coulomb proximity on nuclear decay

S. Hudan, R. Alfaro, L. Beaulieu, B. Davin, Y. Larochelle, T. Lefort, V. E. Viola, H. Xu, R. Yanez, and R. T. de Souza
Department of Chemistry and Indiana University Cyclotron Facility, Indiana University, Bloomington, Indiana 47405, USA

R. J. Charity and L. G. Sobotka
Department of Chemistry, Washington University, St. Louis, Missouri 63130, USA

T. X. Liu, X. D. Liu, W. G. Lynch, R. Shomin, W. P. Tan, M. B. Tsang, A. Vander Molen, A. Wagner, and H. F. Xi
National Superconducting Cyclotron Laboratory and Department of Physics and Astronomy, Michigan State University, East Lansing, Michigan 48824, USA

(Received 14 May 2004; published 21 September 2004)

Alpha particles emitted from an excited projectilelike fragment (PLF^*) formed in a peripheral collision of two intermediate-energy heavy ions exhibit a strong preference for emission towards the targetlike fragment. The interplay of the initial deformation of the PLF^* caused by the reaction, Coulomb proximity, and the rotation of the PLF^* results in the observed anisotropic angular distribution. Changes in the shape of the angular distribution with excitation energy are interpreted as being the result of forming more elongated initial geometries in the more peripheral collisions.

DOI: 10.1103/PhysRevC.70.031601 PACS number(s): 25.70.Mn

Emission of α particles and other light clusters from heavy nuclei is traditionally explained as an evaporative process governed by the available excitation energy. In contrast, understanding the fission of a heavy nucleus involves a description of the evolution of collective degrees of freedom (shape) as the nuclear system reorganizes itself from a single nucleus into two heavy nuclei. It has been proposed that thermal shape fluctuations, i.e., deformation, play a significant role in the statistical emission of large clusters [1]. The importance of such thermal fluctuations has recently been incorporated within a multistep statistical model code [2]. One means of generating large deformation is through the non-central collision of two heavy ions at intermediate energies ($20 \leqslant E/A \leqslant 100$ MeV). Following the exchange of mass, charge, and energy between the projectile and target nuclei, an excited projectilelike fragment (PLF^*) and an excited targetlike fragment (TLF^*), which are deformed, are produced. As the two reaction partners separate they undergo decay resulting in final residues referred to as the projectilelike fragment (PLF) and targetlike fragment (TLF). It is important to understand how this decay is impacted by both the initial configuration of the nuclei and their proximity to one another.

Dynamical fragment production, intermediate between the TLF and PLF, has been previously reported and has been associated with neck fragmentation of a transient nuclear system [3–5]. Recent analyses at intermediate energies [6–10] have elucidated some of the essential characteristics of this decay mode. These dynamical decays are clearly distinguished from standard statistical decay of the undeformed PLF^* and TLF^*. These processes [6,7,10] can be viewed in a fluid dynamical perspective as the double neck rupture of a highly deformed dinuclear system [11] and correspond to decay on a short time scale. It has been suggested that the initial configuration may not only be important for decay on a short time scale but may also impact fragment emission on longer time scales [3,9,12]. In this Rapid Communication, we present direct evidence on the importance of the persistence of the initial deformation and its interplay with Coulomb proximity for longer time-scale fragment emission.

In an experiment performed at Michigan State University, we bombarded a ^{92}Mo target foil 5.45 mg/cm^2 thick with ^{114}Cd ions accelerated to $E/A = 50$ MeV by the K1200 cyclotron. A key aspect of this experiment was the detection of a PLF ($15 \leqslant Z \leqslant 46$) at very forward angles ($2.1° \leqslant \theta_{lab} \leqslant 4.2°$) with good angular ($\Delta\theta = 0.13°$, $\Delta\phi = 22.5°$) and energy resolution. Identification of the PLF by the ΔE-E technique provided better than unit resolution, $\delta Z/Z \approx 0.25$. Associated charged particles emitted at larger angles ($7° \leqslant \theta_{lab} \leqslant 58°$) were measured in LASSA, a large area silicon strip array [13,14]. The kinematic coverage in the experiment allowed us to reconstruct the decay of the PLF^* [15]. The excitation of the PLF^*, which is correlated with its velocity damping, was deduced from the measured multiplicities and kinetic energies of the detected particles in a calorimetric analysis [15].

The binary nature of the collisions studied, namely the survival of a PLF^* (and TLF^*) fragment, is presented in Fig. 1. Alpha particles detected in LASSA, coincident with a PLF, are shown in the invariant cross-section map presented in Fig. 1. The dominant feature evident in this figure is an essentially circular ridge of yield centered on the reconstructed PLF^* velocity with a radius that corresponds to the Coulomb repulsion between the emitted α and the PLF^* residue, for a touching spheres configuration. The minimum angle established by the experimental acceptance for α emission ($\theta_{lab} \geqslant 7°$) is indicated by the dashed line. For the remainder of this work we focus on the yield along the Coulomb ridge, which corresponds to a well-defined configuration between the emitted α and PLF^* residue. In addition to standard evaporation from the PLF^*, midvelocity emission [9,16] may also contribute to the yield along the Coulomb ridge evident

 ©2004 The American Physical Society

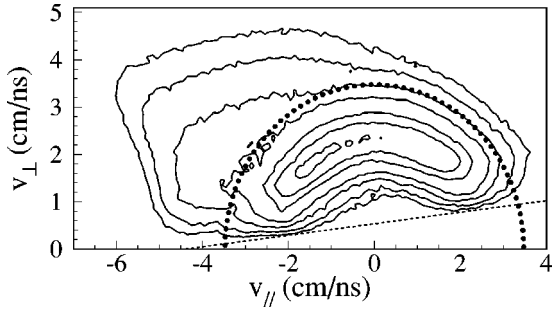

FIG. 1. Invariant cross-section map (linear scale) of α particles in the PLF* frame for the reaction ^{114}Cd+^{92}Mo at $E/A=50$ MeV. The dotted line depicts the energy cut described in the text. The dashed line indicates the minimum angle ($\theta_{lab} \geq 7°$) for detection of α particles.

in Fig. 1. To assess the contribution of midvelocity α emission to the Coulomb ridge we performed Coulomb trajectory calculations which accounted for emission from the PLF*, TLF*, and a midvelocity source. The size ($\langle Z \rangle = 32, \langle A \rangle = 69$), velocity, and temperature ($T=4$ MeV) of the PLF* were chosen to reflect the experimentally observed quantities [15]. The midvelocity source, located at the nucleon-nucleon center-of-mass frame, was assumed to have a ($\langle Z \rangle = 22, \langle A \rangle = 50$) with a temperature of $T=20-30$ MeV. Reasonable choices for the properties of the TLF* do not contribute significant yield to the kinematical region considered. All sources were assumed to emit isotropically with Maxwell-Boltzmann distributions. To reproduce the shape of the kinetic energy spectra for various angles in the PLF* frame, it was necessary to assume that the relative α emission probability of the midvelocity source was twice that of the PLF*. For such conditions, only a small portion ($\approx 10\%$) of the backward yield ($\theta \geq 90°$) along the Coulomb ridge ($E_\alpha \leq 25$ MeV) is attributable to the midvelocity source.

In Fig. 2 the yield of detected α particles with $E_\alpha \leq 25$ MeV (as indicated by the dotted line in Fig. 1), i.e., dominated by the ridge in Fig. 1, is displayed in the PLF* frame. To further define the events under investigation, we have chosen an excitation energy ($\langle E^*/A \rangle \approx 2.35$ MeV and ≈ 2.78 MeV) by selecting on the velocity of the PLF* [15]. For these selected events, the average detected Z_{PLF} is ≈ 34 (≈ 32) at $\langle E^*/A \rangle = 2.35$ (2.78) MeV, while the reconstructed atomic number of the PLF* is on average ≈ 37 (≈ 38). The most notable feature in Fig. 2 is the large forward-backward asymmetry present for the experimental data (open symbols). The data are backward peaked, towards the TLF, with an enhancement factor of $\approx 2.3-2.6$ relative to $\cos(\theta)=0$. The finite acceptance of the experimental setup, evident in Fig. 1, limits the measured angular distribution to the range $-0.85 \leq \cos(\theta) \leq 0.65$. The lower excitation energy data manifests a broader angular distribution as compared to the higher excitation energy data. We have compared this observed anisotropy with the results of the Coulomb trajectory calculation described above. In the multiple isotropic emission source scenario, Coulomb focusing of α particles emitted backward by the PLF* together with midvelocity emission leads to an anisotropy of $dN/d(\cos\theta)=1.3$ at

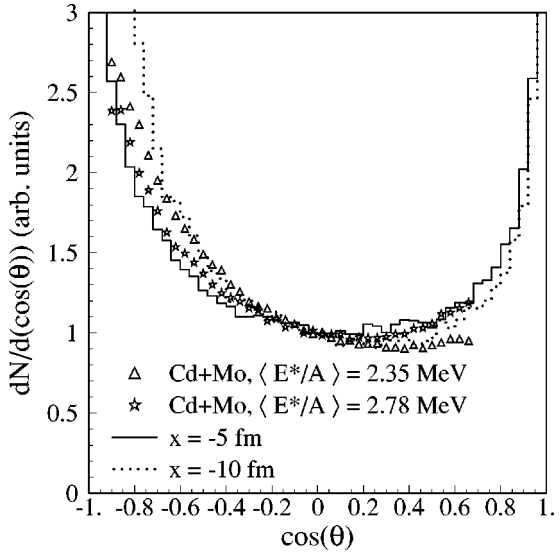

FIG. 2. Comparison of the angular distribution of α particles from the reaction ^{114}Cd+^{92}Mo at $E/A=50$ MeV with $E_\alpha \leq 25$ MeV in the PLF* frame with results of the Langevin model.

$\cos(\theta)=-0.8$ as compared to unity for $\cos(\theta)=0$. Coulomb focusing of PLF* emission due to the presence of the midvelocity source and midvelocity emission are approximately equally responsible for this anisotropy. In short, the Coulomb trajectory calculations demonstrate that the magnitude of the observed anisotropy *cannot* be simply attributed to the joint effect of Coulomb focusing and midvelocity emission. The lines displayed in this figure will be discussed later.

Large backward-forward asymmetries for intermediate mass fragments have been previously observed and have been related to a dynamical fissionlike process [4,6,7,10]. This process, which is characterized by highly aligned decay and relative velocities well above the Viola fission systematics [17], has been related to the neck rupture of a deformed nuclear system. The large relative velocities observed for these aligned decays are believed to be intrinsically related to the collision dynamics. In this work we focus on the asymmetry associated with a simpler configuration, namely one that results in fragments with Coulomb-dominated kinetic energies. To understand the observed asymmetry associated with these simpler configurations we compare the experimental data with the predictions of a one-dimensional Langevin model.

In this schematic model we consider the emission of an α particle from a PLF* ($Z=38$, $A=90$) as it moves away from the TLF*. The emission process of the α particle from the PLF* is governed by a potential which simulates both the nuclear and Coulomb interaction between the α particle and the PLF* residue, as well as their Coulomb interaction with the TLF*. This potential energy is parametrized by

$$V(x) = -(x-c)(x+c)\left(\frac{x}{d}\right)^2 + \sum_{i=1}^{2} e^2 \frac{(Z_{TLF^*})(Z_i)}{R_i}, \qquad (1)$$

where x is the reaction coordinate. The constants c and d, which define the potential, are taken to have values of 12.3

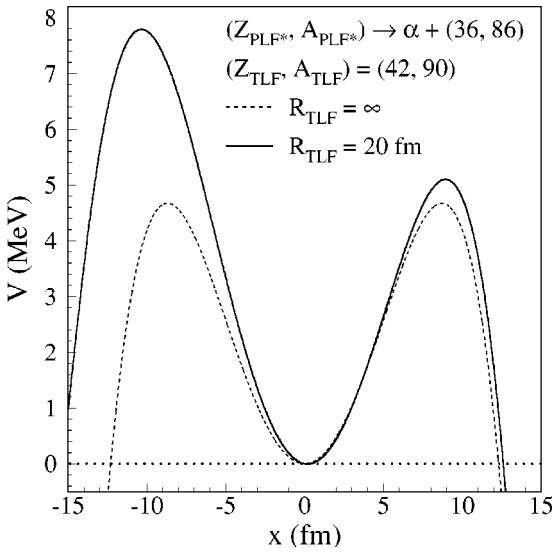

FIG. 3. One-dimensional potential energy diagram of α-particle emission from the PLF* indicating the influence of the TLF* proximity.

and 35, respectively, in order to determine the location of the barriers. The detailed shape of the potential, other than the location of the barriers, has been arbitarily chosen. The second term in the potential describes the interaction of the TLF* with the α particle and PLF* residue with R_1 and R_2 designating the relevant distances. For simplicity, we describe the influence of the TLF* at a distance R_{TLF} from the center of mass of the PLF* system, i.e., $R_{TLF}=R_1-x$. Shown in Fig. 3 is the relative potential normalized so that $V=0$ at $x=0$. When the α particle-residue system decays in isolation ($R_{TLF}=\infty$), the potential is symmetric with a local minimum at $x=0$. Equal height barriers govern backward and forward emission as shown by the dashed line in Fig. 3. For such isolated decay, for an initially undeformed system ($x=0$) forward and backward emission would be equal. The presence of the TLF* at a finite initial distance (e.g., 20 fm) from the α-residue center of mass modifies the potential through its Coulomb influence, increasing the backward barrier more than the forward barrier. A slight outward shift in the barrier positions is also evident in Fig. 3 as indicated by the solid line. For a system with an initially spherical configuration ($x=0$) this asymmetry in the barriers favors forward emission. The experimentally observed yield enhancement in the backward direction therefore suggests that the system is initially deformed towards the TLF*. This initial deformation may originate from the nuclear collision process. As the TLF* and PLF* separate, the Coulomb proximity effect is diminished leading to equal height barriers for forward and backward emission. At a TLF*-PLF* separation distance of 50 fm, the two barriers are essentially equal, corresponding to a sensitivity for time up to $\approx$5 zs (1 zs$=1\times10^{-21}$ s).

This approach to α emission follows a transition state method similar to the way symmetric fission is generally treated. For values of the reaction coordinate x beyond the saddle point, the coordinate can be viewed as the separation distance between the α particle and the center of mass of the α-PLF* residue system in which both α and PLF* residue are taken as spherical. On the other hand, as preformation of the α is not considered, the meaning of the coordinate inside the saddle point should be taken as a generalized reaction coordinate. Nonequilibrium population of this coordinate could, for example, be the trailing tail of nuclear material observed in transport models.

To describe the evolution of an initial configuration as the PLF* moves away from the TLF*, the schematic model utilizes a Langevin approach. The observed angular asymmetry suggests the persistence of the initial configuration. This indicates that the motion is overdamped rather than underdamped; the latter would give rise to forward-backward oscillations of the configuration, resulting in both forward and backward peaking of the angular distribution. Consequently, we work within the high friction limit which allows us, in this schematic model, to eliminate inertial terms. From an initial position on the potential, the change in position of the α particle is given by

$$\Delta x = \frac{F\Delta t}{\beta} + k\sqrt{\frac{2T\Delta t}{\beta}}, \tag{2}$$

where Δt is a time step of 0.1 zs. The first term describes the influence of the potential on the particle's motion with the force due to the potential represented by F, while β corresponds to the friction. The impact of thermal motion on the particle's trajectory is included in the second term. The fluctuating term k is taken to be a Gaussian of unit width centered on zero with the magnitude of the thermal motion scaled for each time step by the temperature T and the friction β. The center of mass of the PLF* and its decay products is conserved at all times.

From its original position on the potential the position of the α is allowed to evolve in time. If the α particle surpasses either barrier the time is recorded. By calculating the fate of the α particle for several initial cases, the relative yield of backward to forward emission, Y (backward)/Y (forward), is determined. Displayed in Fig. 4, is the dependence of the ratio Y (backward)/Y (forward) on the initial TLF*-PLF* distance, R_{TLF}, for different conditions of initial configuration and friction. The temperature was assumed to be 4 MeV in all cases consistent with the reconstructed excitation energy for the experimental data shown in Fig. 2. For the case of an initially spherical configuration ($x=0$), the ratio Y (backward)/Y (forward) is slightly less than unity and increases slightly with increasing R_{TLF}. This result is a direct manifestation of the preference for forward emission due to the Coulomb proximity effect. For a slightly elongated initial configuration, $x=-5$ fm, Y (backward)/Y (forward) exhibits a near constant value of 1.3–1.4. A larger value of the friction, namely $\beta=0.4$ zs MeV/fm^2, results in a marginally larger value for Y (backward)/Y (forward). For such initial configurations, the α particle is well inside both emission barriers. The independence of the yield ratio on R_{TLF} can be understood if by the time the α particle reaches the top of the barrier, the TLF*-PLF* distance is large and the proximity effect is small. Comparison of the $x=0$ and $x=-5$ fm cases clearly indicates that the magnitude of the ratio being larger than unity is related to the persistence of the initial configu-

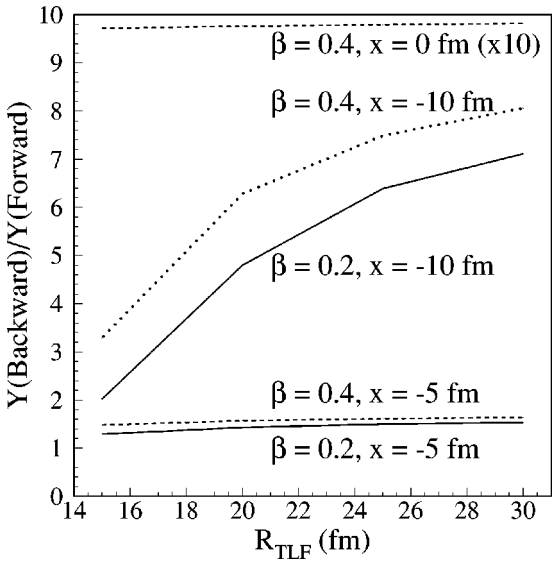

FIG. 4. Yield ratio for backward to forward emission as a function of the initial TLF*-PLF* distance. Calculations for different initial configurations and friction are shown.

ration. If the elongation associated with the initial configuration is large, namely comparable to the barrier position of ≈ -10 fm, then Y (backward)/Y (forward) depends strongly on R_{TLF}. The increase of this ratio with R_{TLF} indicates that the time to overcome the backward barrier is sufficiently short for the Coulomb proximity of the TLF* to be important. For these elongated configurations, an enhanced sensitivity to the friction is also manifested. This enhanced sensitivity to the friction can be understood by considering the motion of the α particle and the change of the potential due to the proximity effect. For elongated configurations, namely a particle near the top of the left barrier, the gradient of the potential is small, resulting in the particle's motion being driven by the thermal term. In the case of larger friction, $\beta = 0.4$, the particle motion is reduced, hence the particle remains near the top of the barrier. As the TLF*-PLF* separate, the importance of the Coulomb proximity is decreased, leading to the decrease in magnitude of the barrier as well as a shift inwards leading to emission of the α particle. In the case of smaller friction, $\beta = 0.2$, the particle initially at the top of the barrier has a 50% probability of moving inward sufficiently so as to be subsequently insensitive to the barrier changes induced by the Coulomb proximity effect. This Langevin approach has also been recently used to explore the importance of the initial distribution on fission transients [18].

The rotation of the decaying PLF* impacts the observed angular asymmetry. If the emission time is longer than a rotational period, a symmetric angular distribution would be observed independent of the initial configuration. The observed angular asymmetry signals that the emission time is short relative to a rotational period. Thus, the measured angular asymmetry presents a "clock" which allows us to measure the time period between the initial separation of the TLF*-PLF* and the emission of the α particle. This scission-to-scission time has previously been investigated and found to depend systematically on the mass asymmetry of the PLF* decay [3]. For the largest mass asymmetries studied, times as short as 0.6 zs were reported. The present case of α-particle emission corresponds to a larger asymmetry than previously investigated. If the α-particle PLF* residue constitutes a rotating dinuclear system, its rotation resembles that of a classical macroscopic object [19]. At lower bombarding energies this relationship between the rotational frequency and the emission lifetime has been used to deduce the fission time scale from the observed angular anisotropy for asymmetric fission [3].

For an assumed spin of the PLF*, the emission time calculated in the model can be related to an emission angle through the rotational frequency. We consider the rotation to be that of two spheres separated by the distance between the α particle and the PLF* residue. One means of ascertaining the spin of the PLF* is through the out-of-plane angular distribution. Unfortunately, limited out-of-plane kinematical coverage in this experiment prohibits us from using this approach. We have therefore assumed, consistent with the out-of-plane widths for similar experiments [3], a spin of $40\hbar$ which corresponds to a rotational period of 3.7 zs. The angular distributions predicted for initial configurations of $x = -5$ fm and $x = -10$ fm are displayed in Fig. 2 as solid and dotted histograms, respectively, for $R_{TLF} = 15$ fm and $\beta = 0.4$. To facilitate comparison of the shape of the predicted angular distribution with the experimentally measured angular distribution, the distributions have been normalized to $\cos(\theta) = 0$. The case of slightly elongated configurations results in a narrower angular distribution at backward angles. Under the assumption of small spin, $10\hbar$ (not shown), the angular distribution is more narrowly peaked at both backward and forward angles, as expected. Moreover, it manifests a lesser dependence on the initial configuration. In this latter case it should be noted that the asymmetry in the total yield still depends strongly on the initial configuration as shown in Fig. 4.

Comparison of the model calculations with the experimental data reveals that under the assumption of a spin of $40\hbar$ the lower excitation energy is better described by $x = -10$ fm while the higher excitation is well described by $x = -5$ fm. In keeping with the schematic nature of the model calculation, no attempt was made to reproduce the detailed shape of the measured angular distributions. As the higher excitation energy corresponds to larger velocity damping of the PLF*, the observed trend suggests that more peripheral collisions are associated with more elongated dinuclear configurations, i.e., more deformed geometries.

While this simple model can provide insight into the interplay of deformation and Coulomb proximity in governing fragment emission, we emphasize that a more complete understanding will require a more realistic multidimensional model, which includes a spin-dependent potential, inertial terms [20] and accounts for the presence of an initial kinetic energy in the emission direction [21] due to incomplete velocity damping in the collision. In addition, the full deexcitation cascade should be accounted for. To allow investigation of small initial separations between the TLF* and PLF*, nuclear proximity effects also need to be incorporated into the model.

Alpha decay of an excited PLF* following a peripheral heavy ion collision at intermediate energy is examined.

Emission in which the fragments manifest predominantly Coulomb kinetic energies exhibits a strongly anisotropic emission pattern, favoring emission toward the TLF^*. This enhancement of backward emission over forward emission can be related to the initial deformation of the PLF^*, induced by the nuclear interaction with the target, and can be affected by the Coulomb interaction between the separating TLF^* and PLF^* system. For large initial deformation, the ratio of backward to forward emission manifests a large sensitivity to the Coulomb proximity effect and to the magnitude of the nuclear friction. The latter must be large in order for the motion to be overdamped. Comparison of the experimental angular distribution with the model calculations indicates that more peripheral collisions are associated with more elongated geometries. Although the nuclear interaction undoubtedly results in a distribution of initial configurations, the simple model presented here captures the essence of the association between the persistence of this initial configurational bias created by the reaction and the observed angular asymmetry.

We would like to acknowledge the staff at MSU-NSCL for providing the high quality beams which made this experiment possible. We gratefully acknowledge several stimulating conversations with A. Sierk on fission dynamics and A. S. Botvina on the topic of the Coulomb proximity effect. This work was supported by the U.S. Department of Energy under, Grant Nos. DE-FG02-92ER40714 (IU), DE-FG02-87ER-40316 (WU) and the National Science Foundation under Grant No. PHY-95-28844 (MSU).

[1] L. G. Moretto, Nucl. Phys. **A247**, 211 (1975).
[2] R. J. Charity, Phys. Rev. C **64**, 064610 (2001).
[3] G. Casini *et al.*, Phys. Rev. Lett. **71**, 2567 (1993).
[4] C. P. Montoya *et al.*, Phys. Rev. Lett. **73**, 3070 (1994).
[5] J. Toke *et al.*, Phys. Rev. Lett. **75**, 2920 (1995).
[6] F. Bocage *et al.*, Nucl. Phys. **A676**, 391 (2000).
[7] B. Davin *et al.*, Phys. Rev. C **65**, 064614 (2002).
[8] S. Piantelli *et al.*, Phys. Rev. Lett. **88**, 052701 (2002).
[9] L. Gingras *et al.*, Phys. Rev. C **65**, 061604(R) (2002).
[10] J. Colin *et al.*, Phys. Rev. C **67**, 064603 (2003).
[11] U. Brosa *et al.*, Phys. Rep. **197**, 167 (1990).
[12] D. Durand *et al.*, Phys. Lett. B **345**, 397 (1995).
[13] B. Davin *et al.*, Nucl. Instrum. Methods Phys. Res. A **473**, 302 (2001).
[14] A. Wagner *et al.*, Nucl. Instrum. Methods Phys. Res. A **456**, 290 (2001).
[15] R. Yanez *et al.*, Phys. Rev. C **68**, 011602(R) (2003).
[16] E. Plagnol *et al.*, Phys. Rev. C **61**, 014606 (2000).
[17] V. E. Viola *et al.*, Phys. Rev. C **31**, 1550 (1985).
[18] R. J. Charity, nucl-th/0406040.
[19] S. Kun, Phys. Lett. B **257**, 247 (1991).
[20] N. Carjan *et al.*, Nucl. Phys. **A452**, 381 (1986).
[21] T. Bredewag *et al.*, Phys. Rev. C **66**, 014608 (2003).